ISSN 0036-0244, Russian Journal of Physical Chemistry A, 2025, Vol. 99, No. 11, pp. 2741–2748. © Pleiades Publishing, Ltd., 2025.

PHYSICAL CHEMISTRY OF DISPERSED SYSTEMS AND SURFACE PHENOMENA

Comparison of Sorption Properties of Reduced Graphene Oxide Aerogels with Soy Wax and Polytetrafluoroethylene

S. A. Baskakov[a,*], Yu. V. Baskakova[a], E. N. Kabachkov[a,b], M. V. Zhidkov[a], A. V. Al'perovich[a], S. S. Krasnikova[a], N. N. Dremova[a], R. I. Usmanov[b], B. E. Antonov[b], and Yu. M. Shul'ga[a]

[a] *Federal Research Center of Problems of Chemical Physics and Medicinal Chemistry, Russian Academy of Sciences, Chernogolovka, 142432 Russia*

[b] *Osipyan Institute of Solid State Physics, Russian Academy of Sciences, Chernogolovka, 142432 Russia*

*****e-mail: baskakov@icp.ac.ru*

Received February 26, 2025; revised February 26, 2025; accepted May 21, 2025

Abstract—Composite aerogels have been produced from reduced graphene oxide (rGO) with polytetrafluoroethylene and soy wax (rGO/PTFE and rGO/wax aerogels, respectively). It has been established that the specific capacity Q_w of the rGO/wax aerogel for solvents, oil, and petroleum products under comparison exceeds that of the rGO/PTFE aerogel. At the same time, the maximum value of the water-wetting angle for a flat surface of the rGO/wax aerogel was 142.4°, whereas this value for the rGO/PTFE aerogel was usually in the range of 161.9°–163.7°. Using the method of differential scanning calorimetry (DSC), it has been shown that the melting point of wax in the rGO/wax aerogel is by approximately 11°C lower than that of pure wax. In addition, the effect of swelling during sorption of solvents has been established for the rGO/wax aerogel. The work has shown among other things that high sorption capacity of material with respect to petroleum products depends not only on its hydrophobicity and oleophilicity, but also on its swelling ~~capacity~~.

Keywords: composite aerogels, reduced graphene oxide, polytetrafluoroethylene, soy wax, hydrophobization, sorption

DOI: 10.1134/S0036024425702231

INTRODUCTION

The most common types of man-caused oil pollution are crude oil, diesel fuel, marine oil, gasoline, and oil condensates. A large number of publications on elimination of oil spills indicate the growing attention to environmental protection [1–13]. Undoubtedly, sorption is an efficient method: sorbents sorb oil in quantities that many times exceed their own weight, converting the oil into a solid or semi-solid state for appropriate disposal or reuse. At present, it is generally accepted that promising synthetic sorbents for eliminating oil spills on water should have, first of all, oleophilic-hydrophobic properties and low specific gravity so as not to sink in water. Sorbents for oil and petroleum products are also characterized by many other parameters: sorption capacity, environmental friendliness, heat resistance, disposal method, reusability, and cost. However, the sorption capacity Q_m is on the first place in development of sorbents. The sorption capacity of such well-known sorbents as sawdust, peat, diatomite, and vermiculite does not exceed 10 g/g. The Q_m value for synthetic sorbents can be as high as 40 g/g (for polypropylene fibers).

Previously, we described a method for producing composite superhydrophobic aerogels of rGO and polytetrafluoroethylene (rGO/PTFE aerogels), for which isopropanol, acetone, and hexane were found to almost completely fill in the free volume of aerogel [14]. High stability of aerogel to cyclic loading with solvents was also demonstrated. In [15], using the sessile droplet method, it was found that the outer surface of rGO/PTFE aerogel is highly hydrophobic, with water-wetting angles of 166°–170°. The porous structure of aerogel granules was studied by the reference contact porosimetry method. The porosimetry curves for octane and water intersect in the region of small pores. This corresponds to the fact that the specific surface area of aerogel with respect to water is much higher than that with respect to octane, although octane is known to wet all materials almost perfectly. This phenomenon is explained by the swelling of sample in water in the region of mesopores because of the hydration of –CO and –COH surface groups. Thus, granules of rGO/PTFE aerogel, which are highly hydrophobic outside, turn out to be hydrophilic inside in the region of small pores, which is a unique phenomenon. No rGO/PTFE aerogel has been tested previously as an oil sorbent.

We have recently developed a simple method for producing a composite rGO/wax aerogel, inexpensive

soy wax used as a hydrophobic additive. The resulting rGO/wax aerogel and an rGO/PTFE aerogel were tested as sorbents for the same solvents. It was the first time when these aerogels were compared as oil sorbents. The sorption capacity of the rGO/wax aerogel for all solvents and oil turned out to be higher than that of the rGO/PTFE aerogel. This served as the basis for a comparative study of aerogels by different physicochemical methods, including comparison of their water-wetting angles.

EXPERIMENTAL

Materials

Soy wax (SW) for container candles was purchased from the Candles Only online store (Russia). Its melting point is 40–50°C; the peroxide value is max 1.0; the free fatty acids: max 0.05; the specific gravity is 0.698–0.921.

Nonionic surfactant Polysorbate 80 (TWIN 80) was purchased in the Mendeleev Shop online store (its quality complies with GOST 32770-2014 "Food additives. Food emulsifiers"). The acid number is 0.94 mg KOH/g; the iodine number is 21.3 g/100 g; the saponification number is 49.4 mg KOH/g; the water ratio is 0.6 wt %; the Gardner color value is 4.5; the hydroxyl number is 66.5 mg KOH/g.

Water suspension F-4D (made by Kirovo-Chepetskaya Khimicheskaya Kompaniya (Kirovo-Chepetsk chemical company) in compliance with TU 6-05-1246-81) was selected as a source of PTFE. The oil sample was taken from tank no. 503 of feed and product storage no. 2 of the commodity production of AO Gazpromneft-MNPZ on November 13, 2020; the solvents were purchased from AO Baza no. 1 Khimreaktivov.

Graphene oxide production

We produced graphene oxide by a modified Hummers method [16]. Details of our method for graphene oxide production are described in [15]. The lateral size of graphene oxide particle was 0.5–5 μm, and the particle thickness was 0.7 to 1.7 nm.

Synthesis of rGO/PTFE aerogel

For preparation of the aerogel, 300 mL of aqueous suspension of graphene oxide (GO) with concentration of 11 mg/mL was placed in a glass beaker and sonicated for 5 min. Next, using a dispenser, the required volume of F-4D suspension was introduced in portions into the GO suspension, without stopping the sonication. After completion of the introduction of the F-4D suspension so that to obtain aerogel with composition of 50 : 50 wt % w.r.t. GO and PTFE, the sonication was continued for another 5 min. In this work, the rGO/PTFE aerogel was produced in the form of a block for the first time. For this purpose, the obtained suspension was frozen in a freezing unit. The unit consists of a glass Dewar vessel, into which a solid copper cylinder with diameter of 50 mm and length of 250 mm is placed. A copper plate measuring 150×150×15 mm is installed on the cylinder. The unit is equipped with an electronic thermometer with a thermocouple to monitor the platform temperature. The operating principle consists in lowering the platform temperature in the Dewar vessel to −80 to −90°C using liquid nitrogen. A pre-fabricated silicone mold for casting a block measuring 100 × 80 × 20 mm was installed on the plate. After freezing, the GO/PTFE hydrogel was removed from the mold and dried for 72 h in an IlShin BioBase FDS5512 freeze dryer (Seoul, Republic of Korea). After drying, the aerogel was subjected to stepwise heat treatment at temperature of up to 360°C for graphene oxide reduction and removal of surfactants from PTFE particles. The aerogel obtained after the heat treatment is hereinafter referred to as rGO/PTFE.

Synthesis of rGO/wax aerogel

The SW suspension was prepared as an "oil in water" one. 21 mL of water, 3 g of soy wax, and 0.5 mL of TWIN 80 were added to a 50-mL beaker. The mixture was thermostatted at 55°C until the wax completely melted, and then dispersed using an MEF 93.1 ultrasonic homogenizer (OOO MELFIZ-ul'trazvuk, Moscow, Russia, ultrasonic intensity of 250 W/cm^2, switching power of 600 W, and operating frequency of 22 kHz) until a milky-white emulsion was obtained. The procedure for producing rGO/wax aerogels was as follows: 150 mL of graphene oxide suspension with concentration of 10 mg/mL was treated with ultrasound for 3 min, and 15 mL of the SW emulsion was added dropwise to it, the ultrasound exposure going on. The ultrasound treatment was continued for another 5 min after the introduction of the SW emulsion was stopped. The resulting dispersion was frozen, as a rule, in 5-mL cylindrical molds mounted on a copper plate being cooled with liquid nitrogen. Note that the freezing molds could be other than cylindrical. After freezing, the hydrogels were removed from the molds and freeze-dried in the IlShin BioBase FD5512 freeze dryer (Seoul, Republic of Korea) at a temperature of −62°C and a pressure of 5 mTorr. The heat treatment of the GO/wax aerogel was carried out with the temperature increased stepwise up to 250°C. The sample was first heated to 100°C and held for 1 h, and then the temperature was raised in steps of 50°C with intervals of 1 h.

Study of sorption properties

The sorption capacity of the aerogels with respect to organic solvents, oil, and petroleum products was studied under static conditions. For this purpose,

approximately 100 mL of solvent, oil, or petroleum product was poured into a test container so that the height of the liquid column was not less than 2.5 cm.

Pre-weighed aerogel was placed in a mesh basket with a lid, and the basket was immersed in the container so that the basket with the aerogel was freely placed inside the container. After 10 minutes, the basket with the aerogel was taken out and was left for the remaining solvent to drain for 1 min. After this, the contents of the basket were transferred to a tray of a known mass. Then the tray with the aerogel was weighed, and the result was recorded.

The sorption capacity (g/g) was calculated by the formula

$$Q_m = m_s/m_a, \quad (1)$$

where m_s is the mass of the sorbed solvent, oil, or petroleum product, g; m_a is the mass of the initial aerogel, g.

The volume fraction (%) occupied by the solvent, oil, or petroleum products was calculated by the formula

$$Q_v = (V_a/V_0)\times 100\%, \quad (2)$$

where V_0 is the volume of the dry aerogel and V_a is the volume of the solvent adsorbed by the aerogel.

Cyclic tests of an rGO/wax aerogel sample in the sorption-desorption mode were also carried out with hexane used for estimation of the possibility of reusing such a sorbent. To this end, a dry sample was weighed, then impregnated in the solvent as described above, and weighed again. Then the sample was dried in a drying oven at $T = 65$°C to constant mass. After the drying, the sample was weighed again. These procedures were taken as one sorption-desorption cycle. In total, ten such cycles were carried out.

Instrumentation

IR spectra (resolution of 4 cm^{-1}; 32 scans) were recorded at room temperature in the range of 4000–450 cm^{-1} with a Perkin Elmer Spectrum Two FTIR spectrometer (Waltham, MA, United States) using an attenuated total reflection (ATR) attachment. Raman spectra were obtained with a Comfotech NR500 Raman microscope (SOL instruments, Minsk, Belarus). The laser excitation wavelength was 532 nm; the power at a measurement point was 0.1 mW; the beam diameter was ~2 μm. Electron micrographs were obtained using a SUPRA 25 scanning electron microscope (Zeiss, Germany) at a chamber pressure of 2×10^{-5} Pa.

DSC curves were recorded using a DSC 822 device (Mettler-Toledo, Spain). Samples weighing 3–5 mg were placed in an aluminum ampoule; during the measurement, the ampoule was in an argon atmosphere at a flow rate of 50 mL/min. The heat release was measured in the temperature range from −10 to +90°C at a minimum heating rate of 10°C per minute.

For measurement of the water-wetting angle (WA, θ) for a flat surface, analysis of the contour of a sessile droplet was performed with an OSA 20 device (DataPhysics Instruments GmbH, Filderstadt, Germany) at room temperature. The results were processed by the Young-Laplace method with consideration of the physical properties of the sessile droplet and the curved surface of the liquid interface using the software of the SCA 20 module from DataPhysics Instruments.

DISCUSSION OF RESULTS

Appearance and specific weight of aerogels

The change in the color of GO/PTFE aerogel during annealing was described in [14]. Note that the color of the GO/wax aerogel (Fig. 1) was darker than that of the GO/PTFE aerogel, which, however, also became almost black after the heat treatment. After annealing, the volume density of the wax-containing aerogel decreased from 20 to 13 mg/cm^3.

Sorption properties

Table 1 shows data on the sorption capacity of the rGO/wax and rGO/PTFE aerogels with respect to a large number of solvents with various chemical structures, including water and oil. In the case of rGO/wax, data were obtained for some petroleum products (white spirit, kerosene, and motor oil). It can be seen that the rGO/wax aerogel excels the rGO/PTFE aerogel in the data presented in the table. Another advantage of the rGO/wax aerogel over the rGO/PTFE aerogel is its easier and more environmentally friendly production process (see Experimental). Note also that $Q_v^a = 101.80$ for isopropanol is not an error—this value has been checked several times. Apparently, during sorption of isopropanol, swelling of the rGO/wax aerogel occurs. It is important to point out the new data on the rather high sorption capacity of the rGO/PTFE aerogel with respect to water. The value obtained confirms the conclusions of [15] on the hydrophilicity of mesopores of the rGO/PTFE aerogel.

IR spectra

The IR spectrum of the rRO/wax aerogel demonstrates characteristic features of both components (Fig. 2a). The wide intense peak with a maximum at 3371 cm^{-1} is due to the stretching vibrations of O–H bonds in GO. In the spectrum of the composite aerogel, one can also see characteristic numerous low-intensity narrow peaks in the region of wax "fingerprints". However, the spectrum of the composite aerogel cannot be described by a simple sum of the

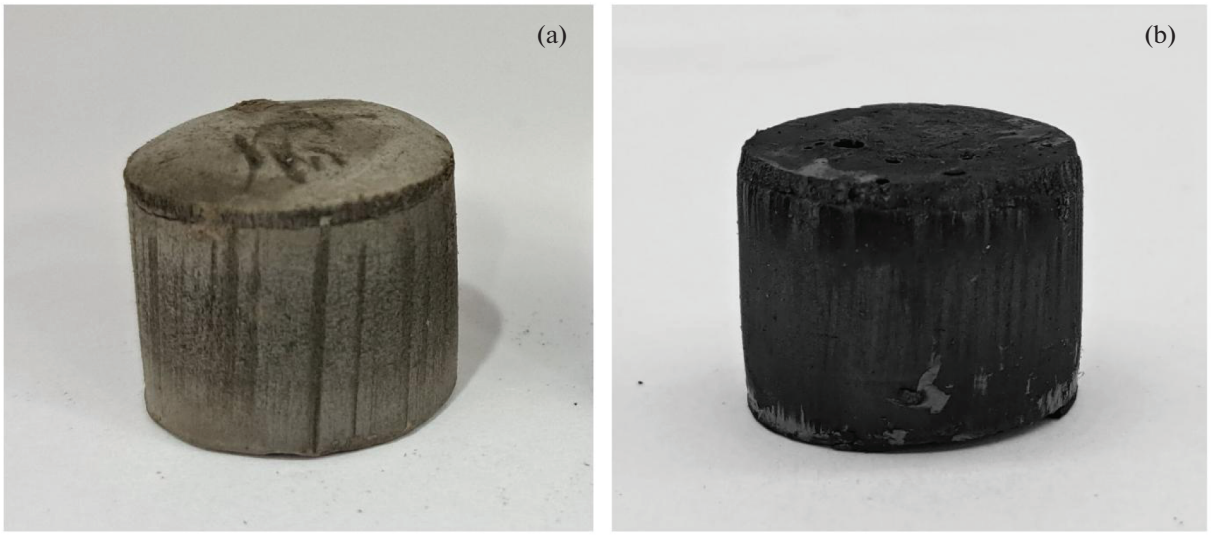

Fig. 1. Photographs of aerogel samples: (a) GO/wax; (b) rGO/wax.

spectra of graphene oxide and wax, because of the presence of a small amount of surfactant and chemical transformations that can occur during the synthesis and drying of the GO/wax aerogel.

For us, it is more interesting to analyze the spectrum of the aerogel after the reduction thermal treatment; i.e., rGO/wax is considered as a target product (Fig. 2, *2*). Primary features of the rGO/wax spectrum are the sloping background and the absence of a wide band of stretching vibrations of O–H bonds and characteristic multiple narrow peaks in the region of wax "fingerprints". These changes indicate a high degree of graphene oxide reduction. The sloping background usually appears in conductive rGO-based samples [17]. The absence of characteristic narrow low-intensity peaks occurred against the position of the most intense wax peaks (2917, 2835, 1736, and 719 cm^{-1}) staying the same. It can be assumed that wax is shielded by conductive rGO sheets.

Table 1. Sorption properties of aerogels

No.	Sorbate	Q_m^a, g/g		Q_v^a, %	
		rGO/wax	rGO/PTFE	rGO/wax	rGO/PTFE
1	Tetrahydrofuran	64.38	23.23[b]	99.91	82.9
2	Toluene	60.70	15.52[b]	96.62	56.6[b]
3	Acetone	52.31	23.15[b]	91.39	94.1[b]
4	Dichlorobenzene	85.83	0.25[b]	91.12	6.20[b]
5	N-hexane	41.86	18.97[b]	87.99	92.5[b]
6	N-heptane	48.58	—	98.68	—
7	Methylpyrrolidone	69.40	—	92.98	—
8	Propanol-2	57.94	23.61[b]	101.80	95.9[b]
9	Petroleum	63.11	17.50	97.85	—
10	Kerosene	53.87	—	87.46	—
11	White spirit	52.43	—	91.59	—
12	Machine oil	56.55	—	91.81	—
13	Water	0.05	2.39	0.06	—

[a] The values presented are defined in the text.
[b] Data from [14].

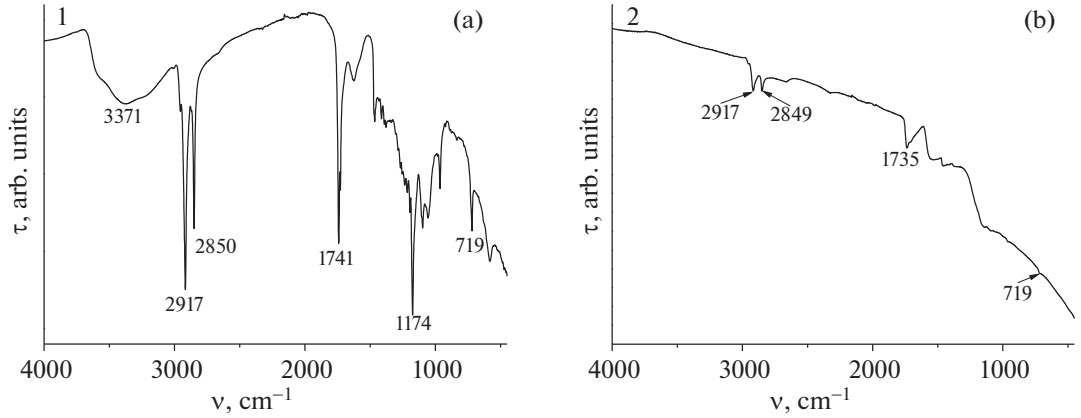

Fig. 2. IR spectra of (a) GO/wax and (b) rGO/wax; ν—wave number, τ—transmittance.

Raman scattering spectroscopy method. Raman scattering spectra

Figure 3 demonstrates Raman scattering (RS) spectra obtained from various points of the rGO/wax aerogel. It can be seen that the main contribution to spectrum 1 (in blue) is given by the peaks with maxima at 1337 and 1578 cm^{-1}, which coincide in their position with peaks *D* and *G* of graphene oxide [18–22]. At the same time, in spectrum 2, apart from peaks *D* and *G,* one can see other, narrower peaks. Some of these peaks, for example, the peak at 1128 cm^{-1}, coincide in their position with the ν_{as}(CC) peak of paraffin [23–26]. One can assume that this point in the area of analysis is occupied mostly by soy wax. Thus, the RS method indicates uneven distribution of the components in the aerogel under study.

Scanning electron microscopy

Figure 4 shows SEM images of the rGO/wax aerogel. It can be seen that graphene oxide sheets form a spatial structure with large interlinked voids. Wax forms both large (200–1000 nm) clumps in folds of GO sheets and small (several nanometers) deposits on the flat surface of these sheets. No such homogeneities were found for the rGO/PTFE aerogel [14].

Differential scanning calorimetry method

It is known that the melting point T_m of fully hydrogenated soybean oil or solid soy wax usually exceeds 60°C [27–29]. In our case, we see two peaks: at 37 and 48°C (Fig. 5). A review of the literature has shown that these values correspond to the melting points of partially hydrogenated or soft soy wax. It should be noted that the literature describes even softer versions of soy wax, on whose differential scanning calorimetry (DSC) curves two peaks were observed, at 25 and 39°C [30]. A small addition of graphene (0.1–1.0 wt %) raises the melting point of pure soy wax by approximately 6°C [31]. In our case, judging only by the maximum, one can say that the melting point of wax in the composite GO/wax aerogel (48°C) has not changed. However, one can also see that the intensity of the T_m = 37°C peak has decreased significantly. As a result of the graphene oxide reduction (transition from GO/wax to rGO/wax), the T_m = 37°C peak becomes the main one in the DSC curve. In the assumption that the low-temperature component (T_m = 37°C) corresponds to the amorphous state of wax and the high-temperature component (T_m = 48°C), to the crystalline state, the transition from GO/wax to rGO/wax should be considered as amorphization of wax due to its spreading over the surface of the GO sheets.

Wetting angle

The water-wetting angle of flat surface of soy wax is 100.5°. In the case of cylinder-shaped GO/wax aero-

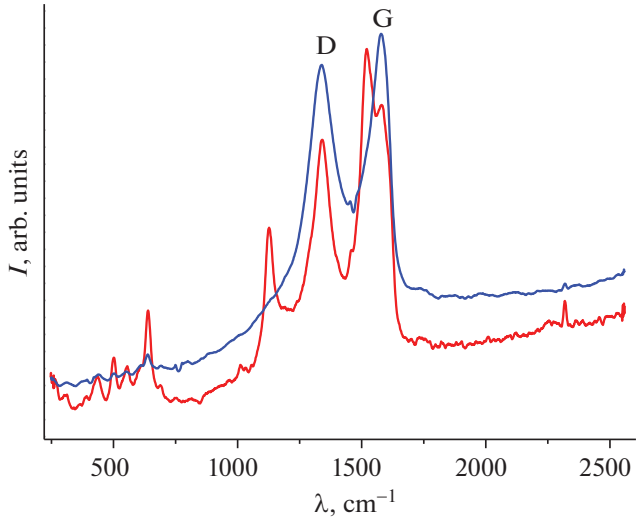

Fig. 3. Raman spectra from different points of rGO/wax aerogel: *I*—intensity, λ—Raman shift.

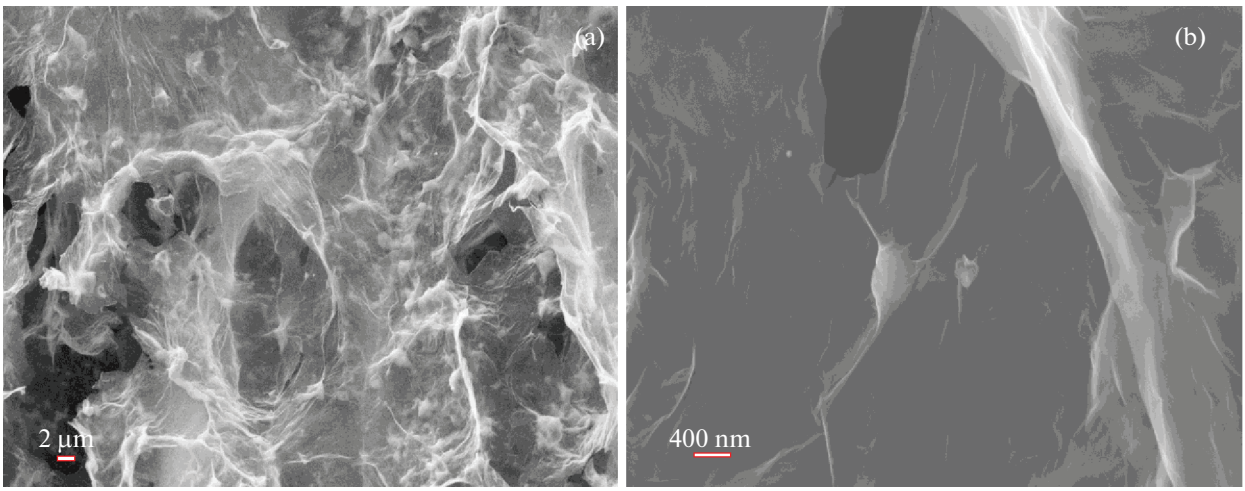

Fig. 4. SEM images of rGO/wax aerogel.

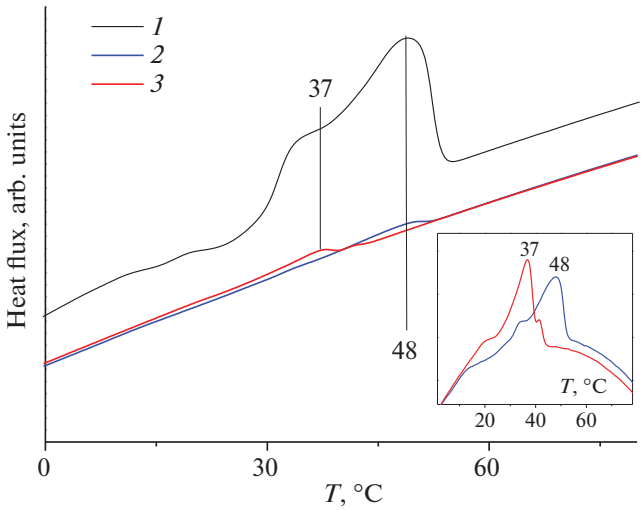

Fig. 5. DSC curves in solid-liquid transition for (*1*) pure wax, (*2*) GO/wax, and (*3*) rGO/wax. Inset: curves for GO/wax and rGO/wax aerogels after deduction of linear background.

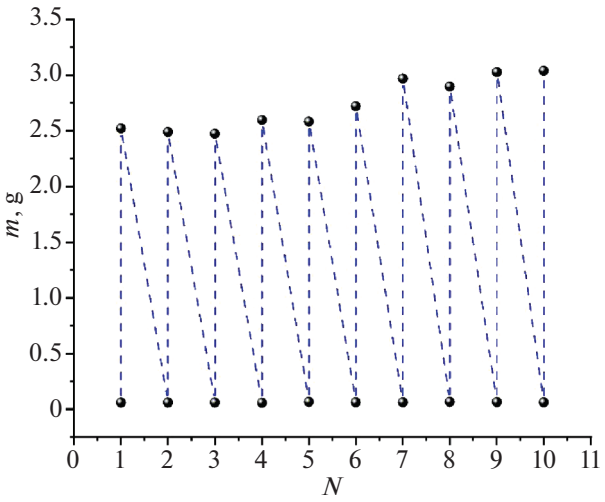

Fig. 6. Cyclic testing of rGO/wax aerogel during hexane sorption-desorption; *m*—sample mass, *N*—cycle number.

gel (Fig. 2), the θ value measured for a flat end surface is significantly higher (136.2°). The annealing procedure increases the wetting angle of the end surface but only up to 142.4°. Note that superhydrophobic graphene aerogel (θ = 151.1°–153.9°) was produced earlier through surface chemical reduction [32]. For the rGO/PTFE aerogel we produced, the θ value was in the range of 161.9°–163.7° [14]. In this respect, the rGO/wax samples obtained in this work are not outstanding, but their hydrophobicity can be considered high enough for an oil sorbent.

Resistance of aerogels to cycling

The resistance of aerogels to sorption-desorption cycles was tested with hexane for both rGO/wax and rGO/PTFE. Figure 6 presents the test results for rGO/wax. The data obtained suggest that both aerogels have high resistance to cyclic loading with the solvent. In the case of rGO/wax, the capacity after the seventh cycle increases by approximately 10%. This means that the aerogel swells during the cycling process; i.e., its volume increases.

The cyclic tests have also shown that the swelling during sorption of hexane occurs differently for different parts of the dry rGO/wax aerogel (Fig.7). After hexane desorption, significant shrinkage of the sample on one of the cylinder bases was observed again, and the sample became like a truncated cone again. These shape changes occurred in each of the ten cycles of sorption tests.

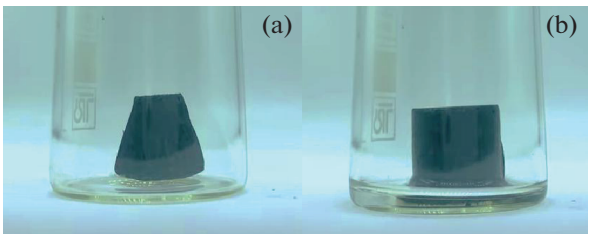

Fig. 7. Photographs of (a) rGO/wax dry aerogel and (b) rGO/wax aerogel impregnated with hexane.

CONCLUSIONS

In this work, composite aerogels with frame of rGO sheets were obtained, a hydrophilic component being either polytetrafluoroethylene (rGO/PTFE aerogel) or wax (rGO/wax aerogel). The sorption properties of the aerogels in relation to solvents, oil, and petroleum products were compared. It has been established that the specific capacity Q_w of the rGO/wax aerogel for all solvents, oil, and petroleum products under comparison exceeds that of the rGO/PTFE aerogel. The most pronounced difference in Q_w was for dichlorobenzene: 85.83 g/g for rGO/wax and 0.25 g/g for rGO/PTFE. At the same time, the maximum value of the water-wetting angle for a flat surface of the rGO/wax aerogel was 142.4°, whereas this value for rGO/PTFE was usually in the range of 161.9°–163.7°. We explain this by the fact that the surface structure of the rGO/PTFE aerogel is different from its volume structure: the surface is more dense and highly hydrophobic, whereas in the volume of the aerogel there are hydrophilic mesopores. This is confirmed by the sorption capacity of the rGO/PTFE aerogel for water (2.39 g/g), which is sorbed through defects on curved parts of the surface of the aerogel. The sorption capacity of the rGO/wax aerogel for water measured under the same conditions is only 0.05 g/g. Both aerogels under comparison withstand at least ten cycles of sorption tests, which implies the possibility of their repeated use in pollution purification systems.

For the rGO/wax aerogel, the effect of swelling during solvent sorption was also revealed. As a result of the work performed, high sorption capacity of material with respect to petroleum products has been shown to depend not only on its hydrophobicity and oleophilicity, but also on its swellability.

FUNDING

This work is supported by the Ministry of Science and Higher Education of the Russian Federation (state assignments 124013000757-0, 124013100858-3, and 124013000692-4).

CONFLICT OF INTEREST

The authors of this work declare that they have no conflicts of interest.

REFERENCES

1. N. Bhardwaj and A. N. Bhaskarwar, Environ. Pollut. **243**, 1758 (2018). https://doi.org/10.1016/j.envpol.2018.09.141
2. L. Bura, A. Woszuk, D. Kołodyńska, et al., Minerals **7**, 37 (2017). https://doi.org/10.3390/min7030037
3. J. Saleem, M. Adil Riaz, and M. Gordon, J. Hazard. Mater. **341**, 424 (2018). https://doi.org/10.1016/j.jhazmat.2017.07.072
4. M. Zamparas, D. Tzivras, V. Dracopoulos, et al., Molecules **25**, 4522 (2020). https://doi.org/10.3390/molecules25194522
5. R. K. Gupta, G. J. Dunderdale, M. W. England, et al., J. Mater. Chem. A **5**, 16025 (2017). https://doi.org/10.1039/C7TA02070H
6. X.-Q. Zhao, F. Wahid, J.-X. Cui, et al., Int. J. Biol. Macromol. **185**, 890 (2021). https://doi.org/10.1016/j.ijbiomac.2021.06.167
7. M. A. Iskar, E. B. Yahya, H. P. S. Abdul Khalil, et al., Polymers **14**, 849 (2022). https://doi.org/10.3390/polym14050849
8. S. Mohammadiun, A. A. Gharahbagh, E. Bakhtavar, et al., J. Hazard. Mater. **463**, 132838 (2024). https://doi.org/10.1016/j.jhazmat.2023.132838
9. S. B. Hammouda, Z. Chen, C. An, et al., J. Clean. Prod. **311**, 127630 (2021). https://doi.org/10.1016/j.jclepro.2021.127630
10. R. Wahi, L. A. Chuah, T. S. Y. Choong, et al., Sep. Purif. Technol. **113**, 51 (2013). https://doi.org/10.1016/j.seppur.2013.04.015
11. J. Ge, H.-Y. Zhao, H.-W. Zhu, et al., Adv. Mater. **28**, 10459 (2016). https://doi.org/10.1002/adma.201601812
12. E. C. Emenike, J. Adeleke, K. O. Iwuozor, et al., J. Water Process Eng. **50**, 103330 (2022). https://doi.org/10.1016/j.jwpe.2022.103330
13. M. Fouladi, M. Kavousi Heidari, and O. Tavakoli, J. Porous Mater. **30**, 1037 (2023). https://doi.org/10.1007/s10934-022-01385-0
14. S. A. Baskakov, Y. V. Baskakova, E. N. Kabachkov, et al., ACS Appl. Mater. Interfaces **35**, 32517 (2019). https://doi.org/10.1021/acsami.9b10455
15. Yu. M. Vol'fkovich, V. E. Sosenkin, N. A. Maiorova, A. Yu. Rychagov, S. A. Baskakov, E. N. Kabachkov, V. I. Korepanov, N. N. Dremova, Yu. V. Baskakova, and Y. M. Shulga, Colloid. J. **83**, 284 (2021). https://doi.org/10.1134/S1061933X21030157
16. W. S. Hummers, Jr. and R. E. Offeman, J. Am. Chem. Soc. **80**, 1339 (1958). https://doi.org/10.1021/ja01539a017
17. Y. M. Shulga, A. V. Melezhik, E. N. Kabachkov, et al., Appl. Phys. A **125**, 460 (2019). https://doi.org/10.1007/s00339-019-2747-x

18. J.-B. Wu, M.-L. Lin, X. X. Cong, et al., Chem. Soc. Rev. **47**, 1822 (2018). https://doi.org/10.1039/c6cs00915h
19. S. Claramunt, A. Varea, D. D. López-Díaz, et al., J. Phys. Chem. C **119**, 10123 (2015). https://doi.org/10.1021/acs.jpcc.5b01590
20. D. López-Díaz, M. López Holgado, J. L. García-Fierro, et al., J. Phys. Chem. C **121**, 20489 (2017). https://doi.org/10.1021/acs.jpcc.7b06236
21. R. G. Abaszade, J. Optoelectron. Biomed. Mater. **14**, 107 (2022). https://doi.org/10.15251/jobm.2022.143.107
22. T. Thanh Doan Nguyen, D. Nguyen, H. Ngoc Doan, et al., Appl. Surf. Sci. **581**, 152325 (2022). https://doi.org/10.1016/j.apsusc.2021.152325
23. A. M. Amorim da Costa, M. P. M. Marques, and L. A. E. Batista de Carvalho, Vibr. Spectrosc. **35**, 165 (2004). https://doi.org/10.1016/j.vibspec.2004.01.004
24. M. Zheng and W. Du, Vibr. Spectrosc. **40**, 219 (2006). https://doi.org/10.1016/j.vibspec.2005.10.001
25. P. Meksiarun, M. Ishigaki, V. A. C. Huck-Pezzei, et al., Sci. Rep. **7**, 44890 (2017). https://doi.org/10.1038/srep44890
26. R. Liu, X. Hu, L. Yang, C. Xie, et al., ACS Omega **8**, 4711 (2023). https://doi.org/10.1021/acsomega.2c06674
27. K. Rezaei, T. Wang, and L. A. Johnson, J. Am. Oil Chem. Soc. **79**, 1241 (2002). https://doi.org/10.1007/s11746-002-0634-z
28. W. Li, X. H. Kong, E. Kharraz, L. Bouzidi, et al., J. Adhesion **87**, 95 (2011). https://doi.org/10.1080/00218464.2011.545286
29. L. Yao, J. Lio, T. Wang, and D. H. Jarboe, J. Am. Oil Chem. Soc. **90**, 1063 (2013). https://doi.org/10.1007/s11746-013-2239-7
30. M. C. Floros, L. Raghunanan, and S. S. Narine, Eur. J. Lipid Sci. Technol. **119**, 1600360 (2017). https://doi.org/10.1002/ejlt.201600360
31. T. Trisnadewi, E. Kusrini, D. M. Nurjaya, et al., IJTech. **14**, 596 (2023). https://doi.org/10.14716/ijtech.v14i3.6092
32. L. Xu, G. Xiao, C. Chen, et al., J. Mater. Chem. A **3**, 7498 (2015). https://doi.org/10.1039/C5TA00383K

Translated by I. Sokolova

SPELL: OK